Water Resour Manage (2013) 27:323–339
DOI 10.1007/s11269-012-0188-9

Streamflow Modeling in a Highly Managed Mountainous Glacier Watershed Using SWAT: The Upper Rhone River Watershed Case in Switzerland

Kazi Rahman · Chetan Maringanti · Martin Beniston · Florian Widmer · Karim Abbaspour · Anthony Lehmann

Received: 27 December 2011 / Accepted: 19 October 2012 /
Published online: 14 November 2012

Abstract Streamflow simulation is often challenging in mountainous watersheds because of irregular topography and complex hydrological processes. Rates of change in precipitation and temperature with respect to elevation often limit the ability to reproduce stream runoff by hydrological models. Anthropogenic influence, such as water transfers in high altitude hydropower reservoirs increases the difficulty in modeling since the natural flow regime is altered by long term storage of water in the reservoirs. The Soil and Water Assessment Tool (SWAT) was used for simulating streamflow in the upper Rhone watershed located in the south western part of Switzerland. The catchment area covers 5220 km^2, where most of the land cover is dominated by forest and 14 % is glacier. Streamflow calibration was done at daily time steps for the period of 2001–2005, and validated for 2006–2010. Two different approaches were used for simulating snow and glacier melt process, namely the temperature index approach with and without elevation bands. The hydropower network was implemented based on the intake points that form part of the inter-reservoir network. Subbasins were grouped into two major categories

K. Rahman (✉) · M. Beniston · A. Lehmann
Institute for Environmental Science, University of Geneva, Geneva, Switzerland
e-mail: kazi.rahman@unige.ch

M. Beniston
e-mail: martin.beniston@unige.ch

A. Lehmann
e-mail: anthony.lehmann@unige.ch

C. Maringanti
Risk Modeling Unit, Zurich Financial Services Ltd., Zurich, Switzerland
e-mail: chetan.maringanti@zurich.ch

F. Widmer
Hydropower Generation, Alpiq Suisse SA, Lausanne, Switzerland
e-mail: florian.widmer@alpiq.com

K. Abbaspour
Swiss Federal Institute for Aquatic Science and Technology, Duebendorf, Switzerland
e-mail: abbaspour@eawag.ch

with glaciers and without glaciers for simulating snow and glacier melt processes. Model performance was evaluated both visually and statistically where a good relation between observed and simulated discharge was found. Our study suggests that a proper configuration of the network leads to better model performance despite the complexity that arises for water transaction. Implementing elevation bands generates better results than without elevation bands. Results show that considering all the complexity arising from natural variability and anthropogenic influences, SWAT performs well in simulating runoff in the upper Rhone watershed. Findings from this study can be applicable for high elevation snow and glacier dominated catchments with similar hydro-physiographic constraints.

Keywords SWAT · Snow melt · Glacier melt · Hydropower · AMALGAM

1 Introduction

Snow and glacier melt runoff from mountains is the main source of water at the regional scale, with downstream processes, such as hydropower based energy production (Viviroli and Weingartner 2004), biodiversity and ecological balance (Brown et al. 2006) , controlled by processes at higher elevations. Many models have been applied to the simulation of snowpack-snowmelt processes in the watershed, ranging from simple temperature-based equations to complex and sophisticated process-based equations (Debele et al. 2010). In mountainous regions, runoff from snow and glacier melt provides streamflow which is often regulated by storage reservoirs (Fig. 2). In Switzerland, especially the south western part of the country, the heterogeneity of elevation together with diverse forest cover and glacier dynamics present unique challenges as well as potential research opportunities to understand mountain hydrological processes. Temperature index models have been the most common approach (Hock 2003) for melt modeling for a number of reasons, among them a reasonable availability of air temperature data, relatively easy interpolation and forecasting possibilities of air temperature, generally good model performance despite their simplicity and computational simplicity. Applications are numerous and include the prediction of melt for operational flood forecasting and hydrological modeling. However, two drawbacks are apparent; firstly, because of temporal resolution, their accuracy decreases; secondly, simulating longer time period and topographic effect such as shading slope and aspect is a hindrance to modeling spatial variability These effects are crucial in mountain areas (Hock 2003). Recent existing studies were conducted in this region, mostly focusing on the evaluation of glacier surface area and glacier melt runoff (Daniel Farinotti1 2011; Farinotti et al. 2009; Huss 2011; Huss et al. 2010; Schaefli et al. 2005; Schaefli and Huss 2011), and impact on hydro peaking in a distributed manner (Meile et al. 2010) . In addition, some studies were carried out for long term forecasts of streamflow based on climate model outputs, but with little detail about physical processes such as snow and glacier melt (Beniston 2010). Therefore the specific objective of this research is to assess the capabilities of a physically-based hydrological model (SWAT) for runoff simulation in the upper Rhone watershed, considering the entire range of complexity that arises from natural variability and human influence, such as long term water storage in the hydropower reservoirs.

2 Study Area

The upper Rhone river located in the south western part of Switzerland originates from the Rhone glacier (Fette et al. 2007). It is 167.5 km long with a drainage basin

of 5220 km^2. According to Meile et al. (2010) 14 % of its land area is covered with glaciers.

Runoff behavior is characterized by two important regimes: the high flow period that occurs in summer due to snow and ice melt; and the low flow period that occurs during the winter. The average precipitation of the basin is observed to be 1435 mm/year (Schaedler and Weingzutner 2001). The upper Rhone is considered as 7 order tributaries; lower orders are illustrated in Fig. 1. Two main characterizations were done in 1930 and 1960 for flood protection for which 91 % of its length were affected. This channeling reduced its original length from 424 km to 251 km (Meile et al. 2010). In total 11 high head hydropower plants are located in the upper Rhone and most of them started functioning between 1951 and 1975. Therefore a shift of natural behavior has been observed in high flow and low flow periods since the construction of these dams due to the long term storage of water which is illustrated in Fig. 2.

Historical discharge data were collected from Swiss meteorological office (FOEN) for upstream (Gletsch) and downstream (Porte du Scex) observation points. Daily discharge data from 1956–2010 for the Gletsch measuring station were analyzed using monthly discharge hydrographs in order to have an idea about the natural behavior of the runoff process. Among other head water catchments, Gletsch was chosen based on the historic data availability of this discharge gauge. Furthermore, 105 years of daily discharge data (from 1905–2010) were collected from Porte du Scex, located downstream close to the entry-point

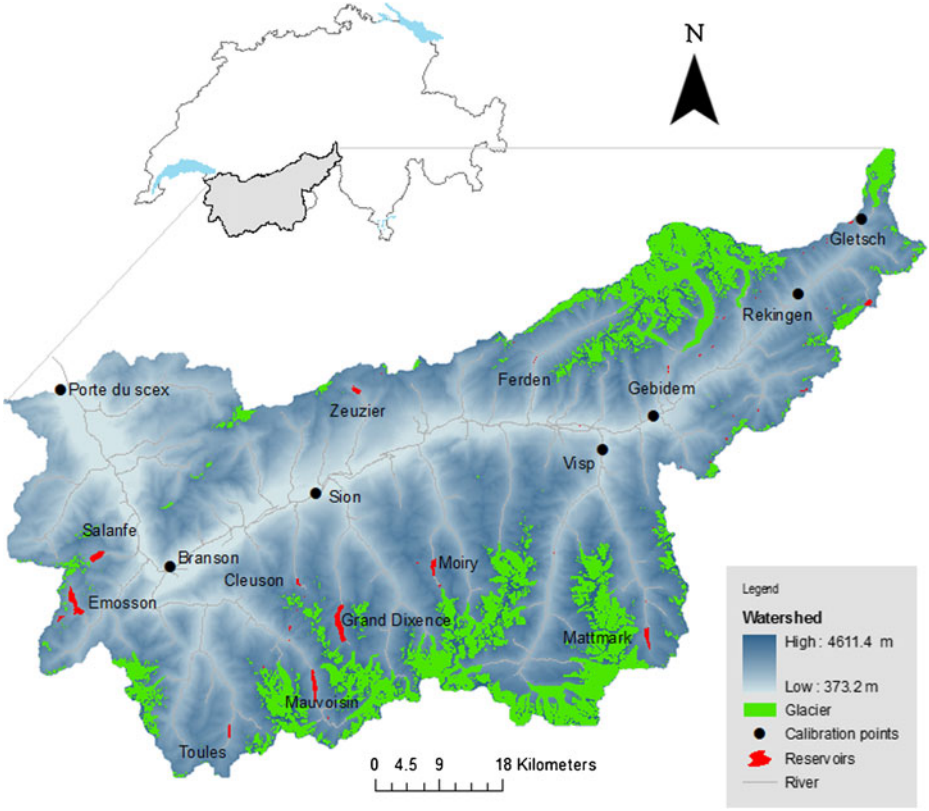

Fig. 1 Upper Rhone river catchment in Switzerland

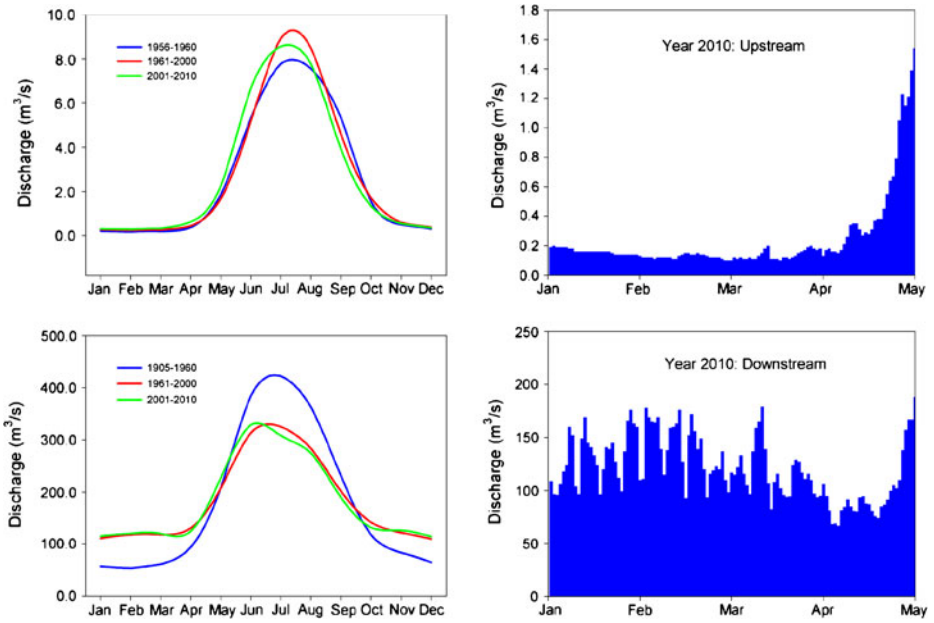

Fig. 2 Upstream [upper left and right] and downstream [lower left and right] discharge comparison. Upper left: Monthly average discharge based on daily discharge record of 1956–2010. Upper right: daily discharge from 1**st** January 2010 to May 2010. Lower left monthly average discharge based on the daily discharge from 1905–2010, lower right daily discharge from 1**st** January to 1st May 2010

into Lake Geneva, where the discharge is a combination of both natural flows and those released from the hydropower reservoirs. A comparison is given in Fig. 2 where the observation line is split into two different time slices for both points. An important observation can be obtained following the years 1960–2000 where the upstream points indicated the higher runoff in the summer period but winter period remained constant, whereas the downstream points illustrated lower runoff in the summer but higher runoff in the winter; this is due to long term storage of water in the hydropower reservoirs which is linked to the energy consumption.

3 Methodology

3.1 SWAT Model

The Soil and Water Assessment Tool (SWAT) Arnold et al. (1998) is a process-based distributed parameter watershed scale simulation model. It subdivides an overall watershed into sub watersheds connected with the river network and smaller units called Hydrological Response Units (HRUs), which each represent a combination of land use, soil and slope. HRUs are non-spatially distributed assuming there is no interaction and dependency (Neitsch et al. 2005). SWAT has been successfully applied all over the world for solving various environmental issues for water quality and quantity studies like diffuse surface water pollution (Panagopoulos et al. 2011; Varanou et al. 2002). But relatively less in snow and glacier dominated mountainous terrain. However, several studies have been performed and a

few studies are ongoing to explore hydrological fluxes in mountain regions (Abbaspour et al. 2007; Ahl et al. 2008; Debele et al. 2010; Fontaine et al. 2002; Morid et al. 2004; Pradhanang et al. 2011; Wang and Melesse 2005; Zhang et al. 2008). The meteorological variables needed to run the model are precipitation, temperature, wind speed, solar radiation, and relative humidity on daily or sub-daily time steps. SWAT simulates energy, hydrology, soil temperature, mass transport and land management at subbasin and HRU level. For this specific study, variables related to discharge and snow melt on mountainous domain will be addressed; more detailed information about the other processes can be obtained from (Neitsch et al. 2005). The hydrological routine of SWAT consists of discharge, snow melt, and evapotranspiration both actual and potential. The SCS curve number method from USDA was used for surface runoff volume estimation. SWAT evaluates evapotranspiration in various methods such as FAO Penman–Monteith, Hargreaves, and Priestley-Taylor. For this study Penman–Monteith was found suitable based on initial model performance before calibration. Data used for the study presented in the Table 1.

3.2 Implementing the Hydropower Network

The built-in command [ROUTRES] in SWAT allows water transfer from one subbasin to another with three different specifications, a fraction of the volume of water in the source, a volume of water left in the source, and the volume of water transferred. In the Rhone watershed, most of the capture points are located downstream of glacier tongues and in most cases all the water is transferred to the reservoir. Based on the site-specific knowledge, geographic coordinates of all the pumping stations were collected and the listed subbasins (Table 2) were used for water transfer. However, it is cumbersome work to modify each of the subbasins affected for pumping station. Also inconsistency may arise for manual operation. In order to avoid inaccuracy a routine was developed in MATLAB considering each of reservoirs inflow outflow scenarios modifying the configuration file (fig.fig) for reservoir routing in SWAT. Several simplifications were made considering the backwater pumping since the water transection does not occur outside of the basin. As an example, hydropower infrastructures are classified into two major groups based on re-pumping of water. Re-pumping mostly occurs when the energy price is high: a compensation pool is used to store the water during high consumption periods and the water is pumped back at

Table 1 Data used and sources

Data Type	Data Sources	Scale	Description
DEM	Swiss-topo	(Grid cell: 25 m · 25 m)	Elevation
Land use	Swiss Federal Statistical Office	(Grid cell: 100 m · 100 m)	Classified land use such as crop, urban forest water etc.
Soil	Swiss Federal Statistical Office	1:200000	Classified soil and physical properties as sand silt clay bulk density etc
Hydro network	Swiss-topo	1:25000	River network-diversion
River flow	FOEN	–	River discharge at daily time step
Weather	Meteo Swiss	–	Precipitation Temperature Wind Speed Solar radiation Wind Speed
Hydropower Discharge	Alpiq, KW Mattmark	–	Inflow and outflow, lake level

Table 2 List of high head hydropower dams with the affected subbasins

Reservoir Name	Volume [mio m^3]	Surface area [ha]	Collecting points	Release points	Reach number
Grande Dixence	401	430	248-150-152-156-157-161-162-166-167-173-174-176-177-178-181-184-186-191-192-193-195-197-204-205-206-207	164	111-114
Emmosson	227	327	153-159-187-208-212-213-216	170	141-123
Mauvoisin	211.5	208	182-185-188-196-198	201	145
Mattmark	101	176	125-128-138-151-155-172-180-168	183	87
Moiry	78	140	106-115-121-127-144	139	64
Les Toules	20.15	61	211-214-219	218	209

night using nuclear power. More details of the networks of water transaction can be obtained from (Hernández 2011; Jordan 2007) (Fig. 3).

Subbasin discretization was achieved using the location of the capture points. The shaded area in Fig. 3 shows the area where natural flow is regulated for storing water in the high-head hydropower reservoirs. Subbasins located inside the shaded area are grouped into one category and the subbasins where natural flow occurs are grouped into another category. Pipe networks and the capacity of pipes were implemented based on a pre-existing study (Frédéric et al. 2007). Discharge information, for instance, inflow to the lake and outflow from the lake was implemented on a daily time step. However it is to be mentioned that some generalization has been done through correlation with energy prices based on long term target levels, since some of the reservoir outflow data were not available.

3.3 Snowmelt Routing Algorithm

Mean daily air temperature is the indicator for precipitation in SWAT, and the boundary temperature (T_{s-r}) is used to categorize precipitation as rain or snow by the user. It is defined in such a way that if the mean daily air temperature is below the boundary temperature, the precipitation will be modeled as snow. Similarly if the temperature is above the boundary temperature, precipitation will be considered to be in the form of liquid rain. Snowfall is stored at the ground surface in the form of an accumulating snow pack, and the amount of water stored there is reported as snow water equivalent. The snow pack will increase with additional snowfall or decrease with snow melt or sublimation. The mass balance for snow pack is

$$SNO = SNO + R_{day} - E_{sub} - SNO_{mlt} \quad (1)$$

Where SNO is the water content of pack on a given day (mm H_2O), R_{day} is the amount of precipitation on a given day (added only if $\overline{T_{av}} \leq T_{s-r}$) (mm of H_2O). E_{sub} is the amount of sublimation on a given day (mm H_2O) and SNO_{mlt} is the amount of snow melt on a given day (mm of H_2O). The snow pack distribution is not uniform over the entire watershed due to large number of influencing factors such as irregular topography, drifting and shading. This results in a fraction of the subbasin area that is bare of snow. This fraction must be computed for the quantification of the snow melt in the subbasin. The factor that contributes to variable snow cover usually has similar values from year to year, making it possible to correlate the areal coverage of snow with the amount of snow present in the subbasin at any given time. For this study, an aerial depletion curve was used to express the seasonal growth

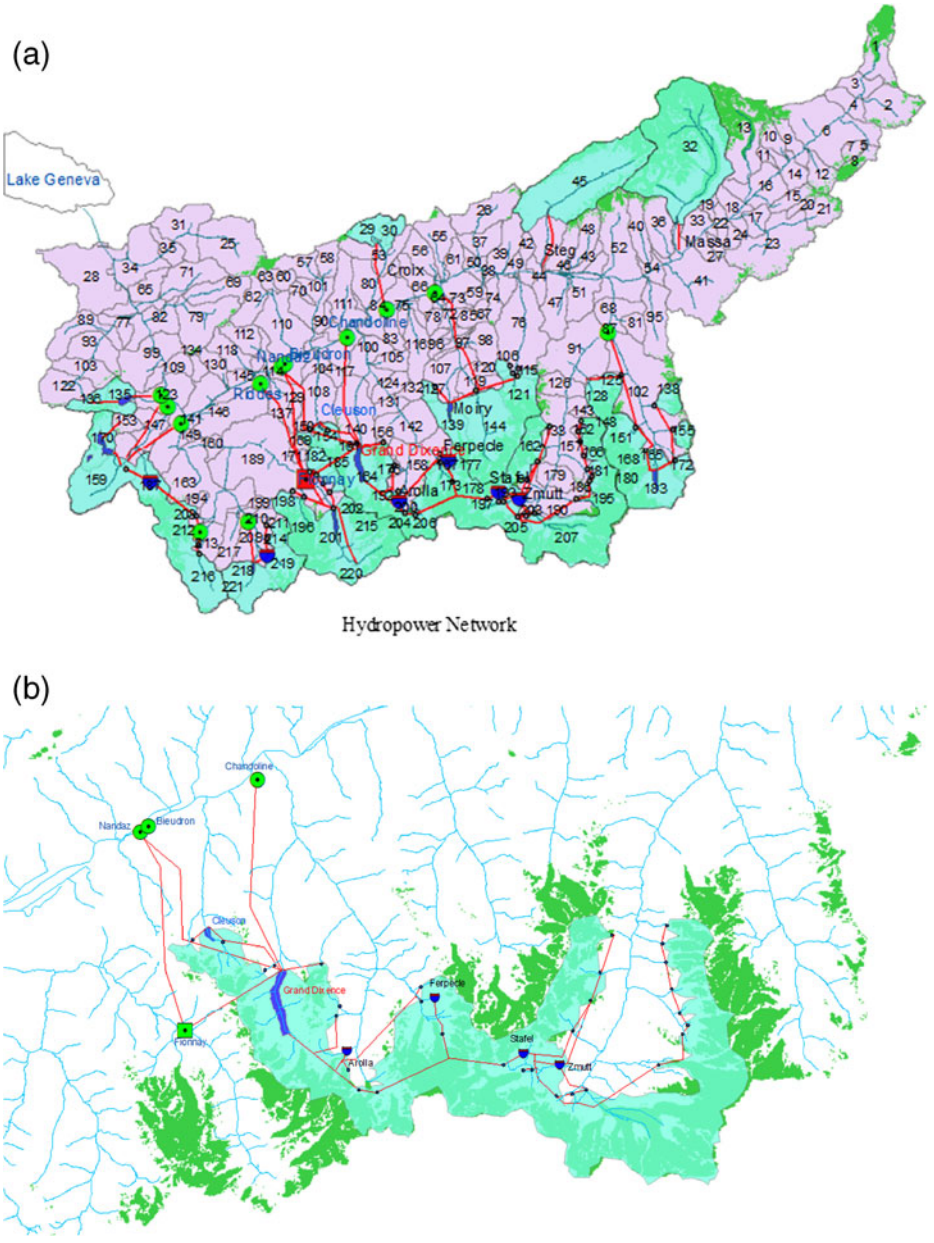

Fig. 3 **a** Hydropower networks of upper Rhone watershed. **b** Hydropower networks of Grande Dixence

and decay of the snow pack as a function of the amount of snow present in the basin. This curve is based on a natural logarithm and is calculated as

$$\mathrm{SNO}_{\mathrm{cov}} = \frac{\mathrm{SNO}}{\mathrm{SNO}_{100}} \times \left[\frac{\mathrm{SNO}}{\mathrm{SNO}_{100}} + \exp\left(\mathrm{cov}_1 - \mathrm{cov}_2 \times \frac{\mathrm{SNO}}{\mathrm{SNO}_{100}}\right)\right]^{-1} \quad (2)$$

Where $\mathrm{SNO}_{\mathrm{cov}}$ is the fraction of HRU area that covered by snow, SNO is the water content of the snow pack on a given day (mm of H_2O), SNO_{100} is the threshold depth of snow at 100 %

coverage (mm of H_2O), cov_1 and cov_2 are coefficients that define the shape of the curve. The values used for cov_1 and cov_2 are determined by solving two known points; these are at 95 % coverage at 95 % SNO_{100} and 50 % coverage at a user specific fraction of SNO_{100}.

3.4 Snow Pack Temperature

The snow pack temperature of current day is calculated using the equation

$$T_{snow(d_n)} = T_{snow(d_n-1)\cdot(1-l_{sno})} + \overline{T_{av}} \cdot l_{sno} \tag{3}$$

where $T_{snow(d_n)}$ is the snow pack temperature on a given day (°C), $T_{snow(d_n-1)}$ is the snow pack temperature on the previous day (°C) l_{sno} is the snow temperature lag factor, and $\overline{T_{av}}$ is the mean air temperature on the current day (°C). As l_{sno} approaches to 1.0, the mean air temperature on the current day exerts an increasingly greater influence on the snow pack temperature while the snow pack temperature from the previous day exerts less and less influence

3.5 Snowmelt Process

The temperature index approach and temperature index with elevation band approach are both used for this case study (Hock 2003). Snow melt is controlled by the air and snow pack temperature, the melting rate and the area coverage of snow. The SWAT model considers melted snow as rainfall in order to compute runoff and percolation. Rainfall energy from the fraction of snow melt is set to zero while computing snowmelt and is estimated assuming uniformly melted snow for 24 hours of the day. Total runoff process explained with the Fig. 4.

3.6 Temperature-index Approach

Temperature is considered as a major controlling factor for snow melt in the temperature index method (Hock 2003). The snow melt in SWAT is calculated as a linear function of the difference between the average snow pack-maximum air temperature and the base or threshold temperature for snow melt

$$SNO_{mlt} = b_{mlt} \cdot sno_{cov} \cdot \left[\frac{T_{snow} + T_{mx}}{2} - T_{mlt}\right] \tag{4}$$

SNO_{mlt} is the amount of snow melt on a given day (mm H_2Ob_{mlt}), is the melt factor for the day (mm H_2O/day-°C), sno_{cov} is the fraction of HRU area covered by snow, T_{snow} is the snow pack temperature on a given day (°C), T_{mx} maximum air temperature on a given day (°CT_{mlt}), base temperature above which snow melt is allowed (°C). The melt factor is allowed seasonal variation with maximum and minimum values occurring on summer and winter solstices

$$b_{mlt} = \left(\frac{b_{mlt6} + b_{mlt12}}{2}\right) + \left(\frac{b_{mlt6} - b_{mlt12}}{2}\right) \times \sin\left(\frac{2\pi}{365}(d_n - 81)\right) \tag{5}$$

Where, b_{mlt} is the melt factor for the day (mm H_2O/day-°C), b_{mltd} is the melt factor for June 21 (mm H_2O/day-°C), b_{mlt12} is the melt factor for December 21 (mm H_2O/day-°C, d_n) is the day number of the year.

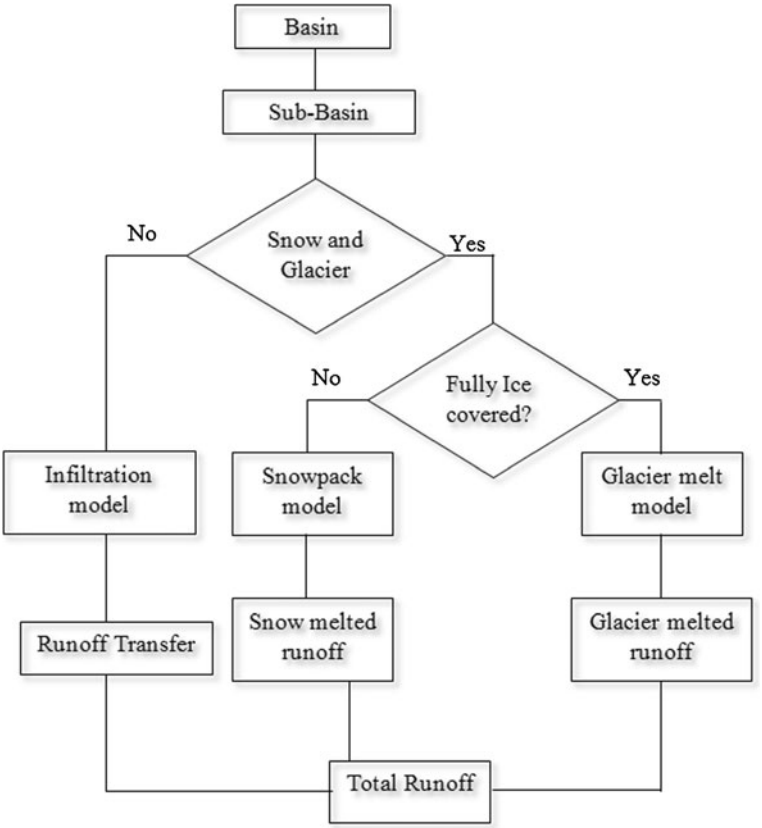

Fig. 4 Schematic diagram of snow and glacier melt process

3.7 Temperature Index with Elevation Band Approach

Elevation is considered one of the very important variables related to meteorological parameters (Zhang et al. 2008), in particular temperature but also snow amount. SWAT allows the sub-basin to be split into a maximum of ten elevation bands, and snow cover and snowmelt are simulated separately for each elevation band (Fontaine et al. 2002). The temperature and precipitation for each band was adjusted using

$$T_B = T + (Z_B - Z) \cdot dT/dZ \tag{6}$$

$$P_B = P + (Z_B - Z) \cdot dP/dZ \tag{7}$$

where T_B is the elevation band mean temperature (°C). T is the temperature measured at the weather station (°C), Z_B is the midpoint elevation of the band(m), Z is the weather station`s elevation (m), P_B is the mean precipitation of the band (mm), P is the precipitation measured at the weather station(mm), dT/dZ is the precipitation lapse reate(mm/km) and dP/dZ is the temperature lapse rate (°C/km). Four elevation bands were set up for the snow and glacier dominated subbasins keeping equal vertical distance from the mean elevation of the centroid

of the subbasins. Snow water equivalents were calculated from the ice thickness map of Huss et al. (2008) based on a contour map of the study area and plugged into each elevation band. Precipitation lapse rate dP/dZ and temperature lapse rate dT/dZ were set to 0.5 mm/km and −0.5 (°C/km) following local lapse rate calculation (Klok et al. 2001).

3.8 Glacier Melt Routing

Subbasins were categorized into two major classes based on the presence of glaciers. The HRUs located within glaciers were treated as solid ice and the glacier information was obtained from (Farinotti et al. 2009). The temperature index approach was used for glacier melt modeling (Hock 2003). In the temperature index model, it is assumed that the melt rate is a linear function of daily positive air temperature. Surface melt rate M is calculated with

$$M = \begin{cases} \left(F_M + r_{ice/snow}\, I\right)T & : T > 0°C \\ 0 & : T \leq 0°C \end{cases} \tag{8}$$

where F_M indicates the melt factor, $r_{ice/snow}$ is the radiation factor of ice and snow. I denotes the clear sky radiation. Daily air temperatures for each elevation band are computed using a lapse rate dT/dZ and similarly precipitation lapse rate dP/dZ also computed assuming a linear increase with elevation.

It is worth mentioning that due to the large number of glaciers, it was not possible to analyze the mass balance of individual glaciers; however, we evaluated the model performance based on the downstream discharge to a large glacier (Rhone Glacier) where a good correlation was obtained with observed flow. (NSE=0.78, R^2=0.82, PBIAS=3.27).

Several sources of uncertainties can be identified when modeling the conceptual snow and glacier melt process. Among these, one can mention the hydrologic model parameterization, orographic effects, the heterogeneity of forest cover, slope, and aspect. These are notable processes that are not well represented by the simple temperature index-driven snow and glacier melt process, and therefore lead to uncertainty in the estimation of glacier-influenced streamflows. Here we focus only parameter uncertainty, our goal was to see whether the parameters follow any specific distribution which is described in the uncertainty section (Fig. 7)

3.9 Model Performance Evaluation

Several studies have proposed a standard hydrological model performance criterion. For this study we followed NSE, PBIAS and R^2 as model evaluation statistics (Moriasi et al. 2007). Model performance were considered satisfactory if NSE>0.5, PBIAS=±25 %. NSE is the strength of the relationship of observed and simulated values where Qm,t is the observed data value at time t and Qs,t is the simulated data value at time t. NSE values lies between −∞ to +1, (Nash and Sutcliffe 1970). Values close to +1 indicates the better model performance.

$$NSE = 1 - \frac{\sum_{t=1}^{T}\left(Q_{m,t} - Q_{s,t}\right)^2}{\sum_{t=1}^{T}\left(Q_{m,t} - \overline{Q}_m\right)^2} \tag{9}$$

$$PBIAS = \left[\frac{\sum_{t=1}^{T}\left(Q_{s,t} - Q_{m,t}\right)}{\sum_{t=1}^{T} Q_{m,t}}\right] \times 100 \tag{10}$$

$$R^2 = \left[\frac{\sum_{t=1}^{T} \left(Q_{m,t} - \overline{Q}_m\right)\left(Q_{s,t} - \overline{Q}_s\right)}{\sum_{t=1}^{T} \left[\left(Q_{m,t} - \overline{Q}_m\right)^2\right]^{0.5} \sum_{t=1}^{T} \left[\left(Q_{s,t} - \overline{Q}_s\right)^2\right]^{0.5}} \right]^2 \quad (11)$$

PBIAS indicates the average tendency of the simulated data to be larger or smaller than their observed value's. According to Gupta et al. (1999), PBIAS can be utilized as an indicator of under- or over-estimation. Negative PBIAS indicates a slight underestimation of model generated values against the measured values. The square of Pearson's product moment correlation is indicated with R^2 which represents the proportions of total variance of measured data that can be explained by simulated data. Higher values of simulated data close to 1 represent better model performance.

4 Results

4.1 Calibration

Our main goal was to evaluate model performance at the most downstream point (Porte du Scex) considering all the complex processes that arise from both natural and human influences. Figure 5 shows the observed and simulated flows at the downstream and upstream points at different phases of calibration. The major problems identified before implementing elevation bands and parameter optimization were that the rising limb of the simulated hydrograph started earlier than the measured hydrograph, and systematic under estimation of both low and high flows of the entire calibration period. Moreover, the simulated hydrograph produced secondary peaks which are not valid in the observed hydrograph. Ultimately, the correlation statistics were also poor (R^2=0.16) (Table 4).

4.2 Manual Calibration

The systematic underestimation problem was solved using the elevation band approach which has results consistent with Fontaine et al. (2002). Several trial and error experiments were made setting up the number of elevation band since SWAT has maximum of 10 bands to set for each subbasin. From the different experiments, we observed that lower numbers with proper configuration of ice thickness result in improved model performance. Similar results have been reported by Pradhanang et al. (2011). Parameter sensitivity was done using the LHOAT technique and the most sensitive parameters were found related to snow melt process. Detailed information about LHOAT can be found in van Griensven et al. (2006). Among the listed selected 9 parameters in Table 3, temperature lapse rate (TLAPS) was found to be the most sensitive, since it is directly related with the melt process of snow and glaciers. The melt factor for snow on June 21 is parameterized by SMFMX, which is responsible for the maximum melt rate ; any increase of this value results in rapid melt. Snow melting process occurs mostly from March to June in the Rhone watershed therefore, the value was adjusted to 3.8 with several trial and error experiments in the manual calibraion process. The snow temperature lag factor TIMP is also linked with SMFMX since it considers the previous days situation. Along with TIMP suface water lag time, SURLAG plays important role for the model performance as the melted snow routing process is related to the geology of the watershed where most of the melted water flows as surface runoff over impervious rock formations. SMTMP is sensitive since it is the indicator of the starting and ending of melt, taking into account the availability of snow for

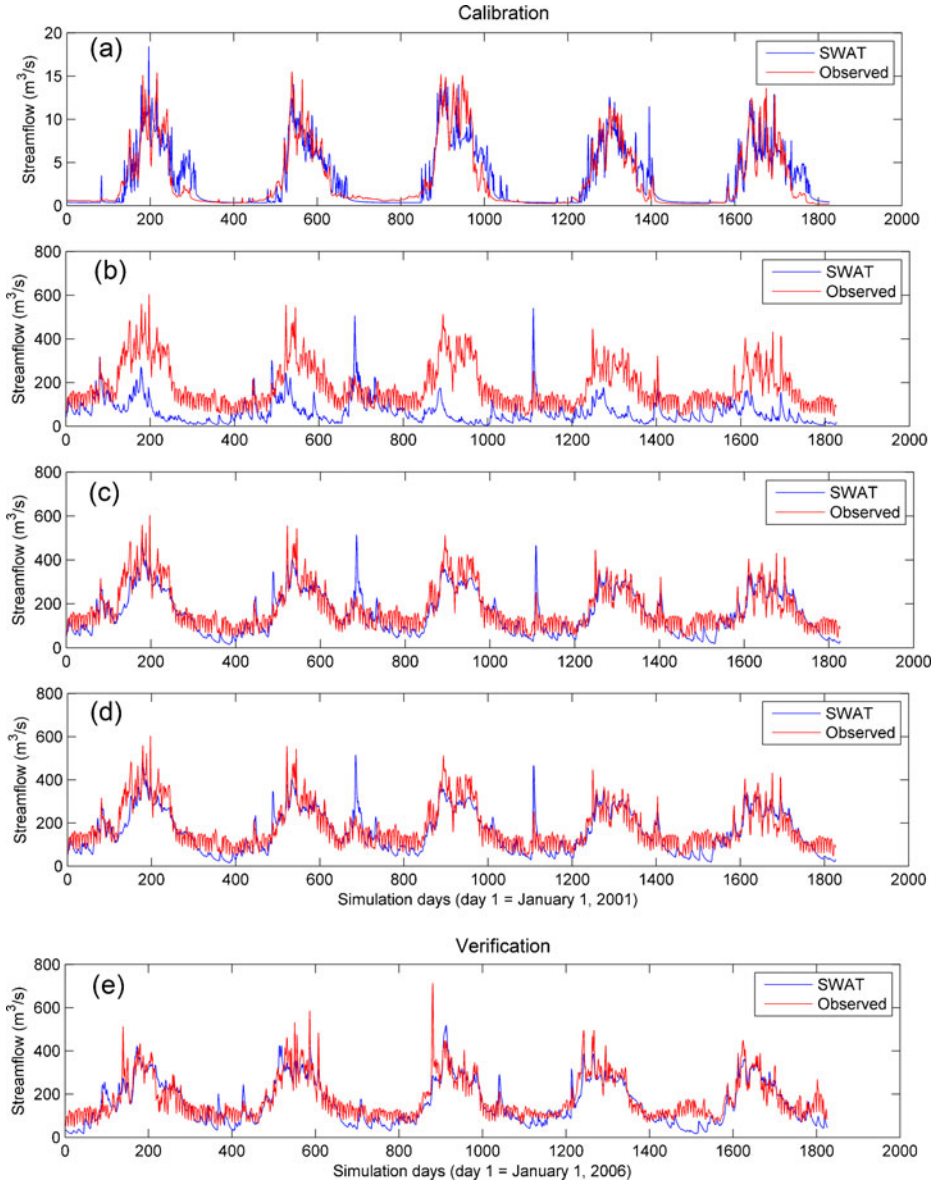

Fig. 5 Observed and simulated relationship for calibration and verification period. **a** Observed and simulated discharge at upstream. **b** Observed and simulated relationship before calibration. **c** Observed and simulated relationship with manual calibration. **d** Observed and simulated relationship with automatic calibration. **e** Observed and simulated relationship at the verification period

melting on a specific day. As a result model-generated streamflow, especially peaks, are significantly influenced by the variation in SMTMP. The snow accumulation process mostly occurs between October and December, and the simulation period was started from January. As a consequence, the initial water content of each elevation band was filled up with SNOEB 150 mm for each elevation band (Table 3).

Table 3 List of calibrated parameters and their optimized value

Parameter	Description	Range	Optimized value
TLAPS	Temperature lapse rate [°C/km]	0,−10	−3.8
PLAPS	Precipitation lapse rate [mm H_2O/km]	0,100	5.8
SFTMP	Snowfall temperature[°C]	−5,+5	1.221
SMTMP	Snow melt base temperature [°C]	−5,+5	2.1
SNOEB	Initial snow water content in elevation band [mm]	0,300	150
TIMP	Snow pack temperature lag factor	0.01,1	1
SMFMN	Melt factor for snow on December 21 [mm H_2O/°C-day]	0,10	2.1
SMFMX	Melt factor for snow on June 21 [mm H_2O/°C-day]	0,10	3.2
SURLAG	Surface runoff lag time [days]	1,4	1

4.3 Automatic Calibration

Automatic calibration was performed for this study in order to optimize the parameter values. Automatic calibration techniques are becoming increasingly popular in hydrological modeling since the iterative procedures can be performed by different algorithms until a possible solution is found. Model parameters were optimized based on the objective function set for model performance (NSE, MSE, and PBIAS). AMALGAM, an automatic calibration technique used for this study which searches for the objective function with the specified set of parameter assigned. AMALGAM comprises four different optimization routines, they are Non-dominated Sorting Genetic Algorithm (NSGA-II) (Deb et al. 2002), Particle Swarm Optimization (PSO), Adaptive Metropolis Search (AMS), and Differential Evolution (DE). Detailed information about AMALGAM can be obtained from Vrugt and Robinson (2007). The parameters obtained from the sensitivity analysis using LH-OAT (van Griensven et al. (2006)) are chosen for automatic calibration. Figure 5(d) is the outcome of 10,000 generations where model performance improved from 0.61 to 0.69 considering NSE as the objective function. Results from the best simulations among the 10,000 generated are plotted in this Figure.

An independent time period was chosen for model verification without changing the parameter values obtained during the calibration period. We selected five years (from 2006–2010) as a verification period in order to test the acceptability of the optimized parameters. Figure 5(d) represents the outcome of the verification period with the statistical performance provided in Table 4. Correlation statistics are represented in the Fig. 6.

4.4 Uncertainty Estimation

Figure 7 represents the frequency distribution of the selected parameters used for calibration using a threshold value of NSE greater than 0.50 from 10,000 generations of AMALGAM. The

Table 4 Model performance evaluation for initial, calibration and verification period

Stages	NSE	R^2	PBIAS
Initial setup	−1.38	0.16	64
Manual calibration	0.61	0.73	5.5
Automatic calibration	0.69	0.81	6.7
Model verification	0.63	0.73	10.23

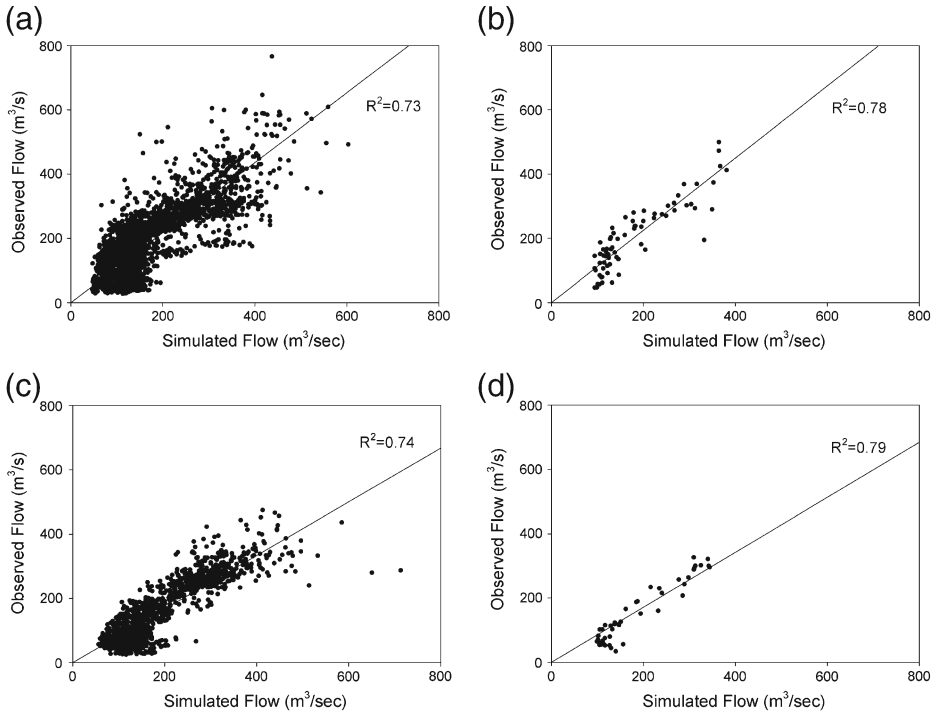

Fig. 6 Co-efficient of determination for calibration and verification period at daily and monthly time steps, upper left and right denotes calibration period lower left and right indicates verification period

y-axis represents parameters and the x-axis represents their ranges. As shown in Fig. 5(e) most of the parameters do not exhibit any specific distribution. However, a sign of normal distribution can be found with the snowfall temperature (SFTMP), which lies between +1 and −1.

Surface water lag time (SURLAG) does not seem to follow any significant distribution, but there is a tendency towards lower values for higher frequencies. This is due to the steep gradient of the slope of the watershed; greater uncertainty of SURLAG indicates that runoff lag time plays a significant role for model performance. Higher frequency of occurrence can be obtained from the SCS moisture curve number (CN_F) between 0 and −0.5, it is to be noted that the frequency distribution of CN_F values were chosen based on percent changes and the remainder are based on absolute changes. The maximum melt factor for snow on June 21 (SMFMX) follows a strongly-skewed distribution with the highest frequency of occurrence lying between 0 and 2. This has a very significant implication since the study area is located in the Northern hemisphere; for the Southern hemisphere it would be considered as the minimum melt factor. The snow pack temperature lag factor (TIMP) followed a bell shaped distribution with a trend of higher values close to 1. It is visible between the parameters related to the precipitation lapse rate (PLAPS) and the temperature lapse rate, PLAPS followed a systematic lower frequency of occurrence on higher values but for TLAPS there is no systematic trend of higher frequency distribution indicating the higher uncertainty of rate of change of temperature. It is obvious that with the change of elevation the temperature will follow a negative trend but there is no significant trend seems the parameter is highly uncertain. In general we have observed that the SWAT model parameters affecting the snow and glacier melt characteristics

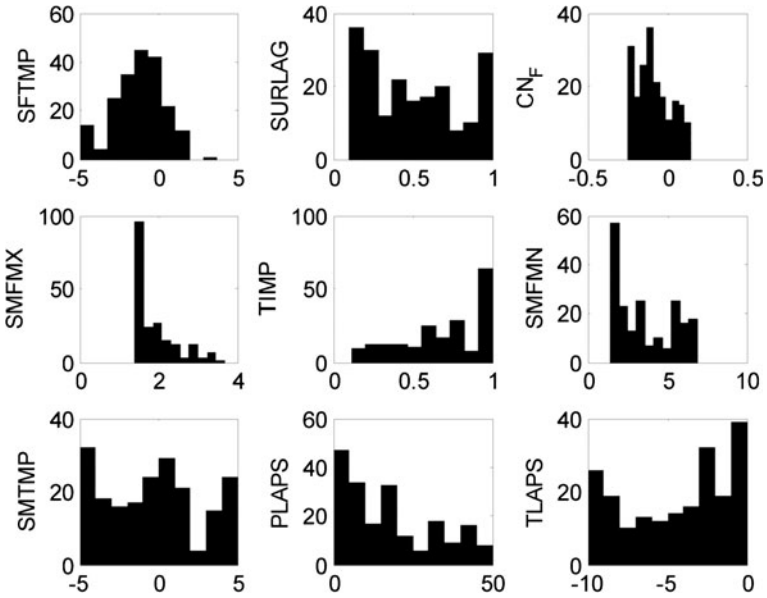

Fig. 7 Frequency distribution of model parameter (NSE>0.5)

were highly uncertain when compared to the surface flow driving parameters. Also it was observed that a different set of SWAT model parameters would lead to similar performance index (NSE in this case) and is termed as equifinality (Beven 2001).

5 Conclusions

This study assessed the performance of the SWAT model's when applied to the complex topography of south-west Switzerland where runoff is a subtle mix of both natural and anthropogenic influences,. The results indicate that, based on the historic discharge analysis (Fig. 2) high-head hydropower storage reservoirs have a very strong influence on the downstream catchments ,which can be modeled with a proper configuration of the affected basin for water transaction. We performed both manual and automatic calibrations; manual calibration were undertaken to understand the hydrological behavior based on the parameter sensitivity, whereas automatic calibrations based on genetic algorithms were performed to obtain the optimal values for a set of iterations. We found relatively better model performance using automatic calibration. The sensitivity analysis indicated that among the 9 parameters considered, snow and glacier melt-related parameters, namely temperature lapse rate, snowmelt temperature, maximum snowmelt factor, and snowpack temperature lag factor, were sensitive for the model performance. The justification is that the temperature index-based snowmelt estimation is seemingly good enough to account for all the physics of snowmelt processes, provided that the calibration parameters are well-adjusted, but application of elevation band with temperature index gives a better understanding of snow and glacier melt processes for different elevation zones. In addition, the model performance statistics improved when using the elevation band approach; as a consequence, it is highly recommended to apply this approach to the case of mountain watersheds. When taking into

account the full range of complexity, the model-generated runoff better matches the observed runoff. Despite the limitation of model performance at the sub-daily scale, information gained from this study may be applied to similar regions of complex terrain in order to assess the impacts of land-use change and climatic change on water availability and use.

Acknowledgment This research was funded by the EU FP7 Project ACQWA (Assessing Climate Change Impact on Water quantity and quality) under Contract No.212250, (http://www.acqwa.ch). We also acknowledge equally the ALPIQ and KW-MATTMARK hydropower companies for providing discharge and lake level data. Coordinates of the intake points were collected from the hydropower consulting engineers E-dric (www.e-dric.ch). We thank anonymous referees for their valuable comments and suggestion for improving our research work.

References

Abbaspour KC, Yang J, Maximov I, Siber R, Bogner K, Mieleitner J, Zobrist J, Srinivasan R (2007) Modelling hydrology and water quality in the pre-ailpine/alpine Thur watershed using SWAT. J Hydrol 333(2–4):413–430. doi:10.1016/j.jhydrol.2006.09.014

Ahl RS, Woods SW, Zuuring HR (2008) Hydrologic Calibration and Validation of SWAT in a Snow-Dominated Rocky Mountain Watershed, Montana, USA. J Am Water Resour Assoc 44(6):1411–1430. doi:10.1111/j.1752-1688.2008.00233.x

Arnold JG, Srinivasan R, Muttiah RS, Williams JR (1998) Large area hydrologic modeling and assessment, Part 1: Model Development. JAWRA 34(1):73–89. doi:10.1111/j.1752-1688.1998.tb05961.x

Beniston M (2010) Impacts of climatic change on water and associated economic activities in the Swiss Alps. J Hydrol. doi:10.1016/j.jhydrol.2010.06.046

Beven K (2001) How far can we go in distributed hydrological modelling? Hydrol Earth Syst Sci 5(1):1–12

Brown LE, Hannah DM, Milner AM, Soulsby C, Hodson AJ, Brewer MJ (2006) Water source dynamics in a glacierized alpine river basin (Taillon-Gabietous, French Pyrenees). Water Resour Res 42(8). doi:10.1029/2005wr004268

Daniel Farinotti1 SU, Matthias Huss2, Andreas Bauder1 and Martin Funk (2011) Runoff evolution in the Swiss Alps: projections for selected high-alpine catchments based on ENSEMBLES scenarios. Hydrolog Process

Deb K, Pratap A, Agarwal S, Meyarivan T (2002) A fast and elitist multiobjective genetic algorithm: NSGA-II. IEEE Trans Evol Comput 6(2):182–197

Debele B, Srinivasan R, Gosain AK (2010) Comparison of process-based and temperature-index snowmelt modeling in SWAT. Water Resour Manag 24(6):1065–1088. doi:10.1007/s11269-009-9486-2

Farinotti D, Huss M, Bauder A, Funk M (2009) An estimate of the glacier ice volume in the Swiss Alps. Global Planet Change 225-231. doi:10.1016/j.gloplacha.2009.05.004

Fette M, Weber C, Peter A, Wehrli B (2007) Hydropower production and river rehabilitation: a case study on an alpine river. Environ Model Assess 12(4):257–267. doi:10.1007/s10666-006-9061-7

Fontaine TA, Cruickshank TS, Arnold JG, Hotchkiss RH (2002) Development of a snowfall-snowmelt routine for mountainous terrain for the soil water assessment tool (SWAT). J Hydrol 262(1–4):209–223

Jordan F, Hernández JG, Dubois J, Boillat J-L (2007) MINERVE Modélisation des Intempéries de Nature Extrême du Rhône Valaisan et de leurs Effets

Gupta HV, Sorooshian S, Yapo PO (1999) Status of automatic calibration for hydrologic models: comparison with multilevel expert calibration. J Hydrolog Eng 4(2):135–143. doi:10.1061/(asce)1084-0699(1999)4:2(135

Hernández G (2011) Flood Management in a Complex River Basin with a Real Time Decision Support System Based on Hydrological Forecasts. THÈSE NO 5093 (2011) Ecole Polytechnique Fédérale de Lausanne

Hock R (2003) Temperature index melt modelling in mountain areas. J Hydrol 282(1–4):104–115. doi:10.1016/s0022-1694(03)00257-9

Huss M (2011) Present and future contribution of glacier storage change to runoff from macroscale drainage basins in Europe. Water Resour Res 47. doi:10.1029/2010wr010299

Huss M, Farinotti D, Bauder A, Funk M (2008) Modelling runoff from highly glacierized alpine drainage basins in a changing climate. Hydrolog Process 22(19):3888–3902. doi:10.1002/hyp. 7055

Huss M, Jouvet G, Farinotti D, Bauder A (2010) Future high-mountain hydrology: a new parameterization of glacier retreat. Hydrol Earth Syst Sci 14(5):815–829. doi:10.5194/hess-14-815-2010

Jordan F (2007) Modèle de prévision et de gestion des crues optimisAtion des opérations des aménagements hydroélectriques à accumulation pour la réduction des débits de crue. THÈSE NO 3711 (2007) Ecole Polytechnique Fédérale de 431 Lausanne

Klok EJ, Jasper K, Roelofsma KP, Gurtz J, Badoux A (2001) Distributed hydrological modelling of a heavily glaciated Alpine river basin. Hydrolog Sci J 46(4):553–570

Meile T, Boillat JL, Schleiss A (2010) Hydropeaking indicators for characterization of the Upper-Rhone River in Switzerland. Aquat Sci 1-12. doi:10.1007/s00027-010-0154-7

Moriasi DN, Arnold JG, Van Liew MW, Bingner RL, Harmel RD, Veith TL (2007) Model evaluation guidelines for systematic quantification of accuracy in watershed simulations. Transactions of the Asabe 50(3):885–900

Morid S, Gosain AK, Keshari AK (2004) Response of different snowmelt algorithms to synthesized climatic data for runoff simulation. J Earth Space Phys 30(1):1–9

Nash JE, Sutcliffe JV (1970) River flow forecasting through conceptual models part I—A discussion of principles. J Hydrol 10(3):282–290. doi:10.1016/0022-1694(70)90255-6

Neitsch SL, Arnold JG, Kiniry J, Williams JR (2005) Soil and water assessment tool theoretical documentation, USDA Agricultural Research Service and. TexasA&MBlackland Research Center, Temple

Panagopoulos Y, Makropoulos C, Mimikou M (2011) Diffuse surface water pollution: driving factors for different geoclimatic regions. Water Resour Manag 25(14):3635–3660. doi:10.1007/s11269-011-9874-2

Pradhanang SM, Anandhi A, Mukundan R, Zion MS, Pierson DC, Schneiderman EM, Matonse A, Frei A (2011) Application of SWAT model to assess snowpack development and streamflow in the Cannonsville watershed, New York, USA. Hydrolog Process. doi:10.1002/hyp. 8171

Schaedler B, Weingzutner R (2001) Components of the natural water balance 1961–1990. Hydrological Atlas of Switzerland, Plate 63, Department of Geography, Bern University—Hydrology & Swiss Federal Office for Water and Geology, Bern, Switzerland (in German, French and Italian)

Schaefli B, Huss M (2011) Integrating point glacier mass balance observations into hydrologic model identification. Hydrol Earth Syst Sci 15(4):1227–1241. doi:10.5194/hess-15-1227-2011

Schaefli B, Hingray B, Niggli M, Musy A (2005) A conceptual glacio-hydrological model for high mountainous catchments. Hydrol Earth Syst Sci 9(1–2):95–109

van Griensven A, Meixner T, Grunwald S, Bishop T, Diluzio A, Srinivasan R (2006) A global sensitivity analysis tool for the parameters of multi-variable catchment models. J Hydrol 324(1–4):10–23. doi:10.1016/j.jhydrol.2005.09.008

Varanou E, Gkouvatsou E, Baltas E, Mimikou M (2002) Quantity and quality integrated catchment modeling under climate change with use of soil and water assessment tool model. J Hydrolog Eng 7(3):228–244. doi:10.1061/(asce)1084-0699(2002) 7:3(228

Viviroli D, Weingartner R (2004) The hydrological significance of mountains: from regional to global scale. Hydrol Earth Syst Sci 8(6):1016–1029

Vrugt JA, Robinson BA (2007) Improved evolutionary optimization from genetically adaptive multimethod search. Proc Natl Acad Sci U S A 104(3):708–711. doi:10.1073/pnas.0610471104

Wang X, Melesse AM (2005) Evaluation of the swat model's snowmelt hydrology in a northwestern Minnesota watershed. Trans ASAE 48(4):1359–1376

Zhang XS, Srinivasan R, Debele B, Hao FH (2008) Runoff simulation of the headwaters of the Yellow River using the SWAT model with three snowmelt algorithms. J Am Water Resour Assoc 44(1):48–61. doi:10.1111/j.1752-1688.2007.00137.x